

OPEN ACCESS

EDITED BY Domenico Albano, University of Brescia, Italy

REVIEWED BY
Carmelo Caldarella,
Fondazione Policlinico Universitario A.
Gemelli IRCCS, Italy
Susovan Jana,
National Institute of Mental Health (NIH),
United States

*CORRESPONDENCE
Xin Li

☑ lixin16@sdu.edu.cn

RECEIVED 06 May 2025 ACCEPTED 08 September 2025 PUBLISHED 19 September 2025

CITATION

Zhou Y, Li K, Jin X, Yuan L, Zhou H and Li X (2025) Imaging findings for 2-[18F] fluoro-2-deoxy-D-glucose positron emission tomography/computed tomography in blastic plasmacytoid dendritic cell neoplasm: case series and literature review. Front. Med. 12:1581760. doi: 10.3389/fmed.2025.1581760

COPYRIGHT

© 2025 Zhou, Li, Jin, Yuan, Zhou and Li. This is an open-access article distributed under the terms of the Creative Commons
Attribution License (CC BY). The use, distribution or reproduction in other forums is permitted, provided the original author(s) and the copyright owner(s) are credited and that the original publication in this journal is cited, in accordance with accepted academic practice. No use, distribution or reproduction is permitted which does not comply with these terms.

Imaging findings for 2-[18F] fluoro-2-deoxy-D-glucose positron emission tomography/computed tomography in blastic plasmacytoid dendritic cell neoplasm: case series and literature review

Yujing Zhou¹, Kaiyue Li¹, Xin Jin², Lujie Yuan¹, Hang Zhou¹ and Xin Li¹*

¹Department of Nuclear Medicine, Qilu Hospital of Shandong University, Jinan, Shandong, China, ²Imaging Center, Jinan Third People's Hospital, Jinan, Shandong, China

Blastic plasmacytoid dendritic cell neoplasm (BPDCN) is a rare hematologic malignancy with a poor prognosis. The value of 2-[18F]fluoro-2-deoxy-D-glucose positron emission tomography/computed tomography (18F-FDG PET/CT) in BPDCN has not been clarified. This study aimed to investigate the imaging findings of ¹⁸F-FDG PET/CT in patients with BPDCN based on cases from our institution and the literature. The clinical and radiological data were obtained from five patients with BPDCN from our institution between March 2014 and July 2023. Additionally, we complemented our dataset with 13 cases derived from the studies published in English to ascertain the potential efficacy of ¹⁸F-FDG PET/CT scan in identifying this malignancy. Information collected included age, sex, extent of lesion involvement, biopsy site, karyotype, immunophenotype, treatment, prognosis, and ¹⁸F-FDG PET/ CT-features. A total of 18 cases of BPDCN featuring PET/CT manifestations were assessed. We observed considerably increased ¹⁸F-FDG uptake in lesions of all 18 cases [maximum standardized uptake value (SUV $_{max}$), 9.1; range, 1.5–9.1]. The positive findings of ¹⁸F-FDG PET/CT mainly included skin (11/18), lymph nodes (9/18), bone (4/18), and spleen (2/18). Except for these organs, abnormal ¹⁸F-FDG uptake lesions were detected in the lung and breast. The roles of ¹⁸F-FDG PET/ CT in our study were initial staging (18/18), selection of biopsy site (5/18), and treatment evaluation (7/18). Prognostic data were available in 16 patients. The median overall survival (OS) in this cohort was 12.0 months, and the median follow-up time was 10.0 months. Among these, 10 cases reported SUV_{max} of lesions at the same time. Five out of eight patients with $SUV_{max} > 2.5$ died within 2 months of diagnosis, whereas two other cases with SUV_{max} < 2.5 survived within 10 and 34 months of follow-up. The data from our case series and those from the literature demonstrated the potential utility of ¹⁸F-FDG PET/CT in diagnosis, staging, prognosis, and treatment follow-up of BPDCN. Early identification of this rare malignancy on imaging can expedite diagnosis and facilitate early treatment.

KEYWORDS

blastic plasmacytoid dendritic cell neoplasm, ¹⁸F-FDG PET/CT, hematologic malignancy, imaging manifestations, prognosis

Introduction

Blastic plasmacytoid dendritic cell neoplasm (BPDCN) is a rare hematologic malignancy with a poor prognosis (1). BPDCN was classified as a distinct clinical entity within the myeloid class of neoplasms in 2016 by the World Health Organization (2). The disease may occur at any age, but most patients are in their sixth or seventh decade of life (3). BPDCN commonly presents as cutaneous lesions, systemic dissemination involving lymph nodes, bone marrow, and extranodal lesions. Laribi et al. (4) reported 398 patients diagnosed with BPDCN. The involvement of the skin, bone marrow, lymph nodes, and peripheral blood at diagnosis was observed in 89, 62, 39, and 15% of cases, respectively. Although infiltrations of extranodal localizations were rare, cases involving the central nervous system (5), ocular adnexa (6), lung (7), breast (8), and uterus (9) were reported. Pathological diagnosis of BPDCN relies on the expression of molecular markers CD4, CD56, and CD123, along with negativity for lineage-specific markers. Furthermore, other markers restricted to plasmacytoid dendritic cells can be positive. However, certain rare cases may lack CD56 (4). Given that the treatment options chosen vary depending on the location of the lesion, it is vital to evaluate the overall condition of patients and the extent of disease involvement at first diagnosis.

The development of positron emission tomography (PET) was a milestone in the development of modern imaging technology. At present, it, combined with computed tomography (CT), reveals metabolic function through the uptake of the radionuclide-labeled probe (10). Increasing evidence indicates that 2-[18F]fluoro-2-deoxy-D-glucose PET/CT (18F-FDG PET/CT) is feasible for assessing pretreatment staging, detecting organ infiltration, and evaluating the treatment response in hematologic malignancy (11). As BPDCN involves multiple systems, 18F-FDG PET/CT may offer an ideal method to observe the glucose metabolism of the whole body in a single examination. Although 18F-FDG PET/CT is used in the clinical treatment of BPDCN, few scholars have reported PET/CT features of the disease.

This study presented five cases of BPDCN from our institution and discussed the potential utility of ¹⁸F-FDG PET/CT in BPDCN in a literature review. It is pertinent to underscore that this retrospective study was carried out in accordance with the Declaration of Helsinki (2000) of the World Medical Association. The study received approval from the ethics committee of Qilu Hospital at Shandong University. Informed consent forms were signed by all participants or their next of kin. We aimed to summarize the role of ¹⁸F-FDG PET/CT in observing organ involvement, guiding biopsies, and assessing the response to chemotherapy in BPDCN treatment.

Case presentation

Case report 1

An 82-year-old man visited our dermatological department with complaints of nodular violaceous rash scattered on the skin of his arm, chest, and back for 2 months. His past medical history included hypertension and type 2 diabetes. The physical examination revealed multiple 3.0- to 5.0-cm nodules in his arms, chest, and back. No palpable lymphadenopathy or hepatosplenomegaly was reported. A

complete blood count revealed mild normochromic normocytic anemia. No abnormalities were detected in the bone marrow aspirate and trephine biopsy. Skin biopsy from the back confirmed the disease as BPDCN. $^{18}\mbox{F-FDG}$ PET/CT revealed multiple mild FDG-avid cutaneous lesions on the arm, chest, and back with an SUV $_{\mbox{\scriptsize max}}$ of 1.5 (the SUV of the liver was measured as 2.6). The patient is currently receiving the first cycle of chemotherapy with azacitidine and venetoclax.

Case report 2

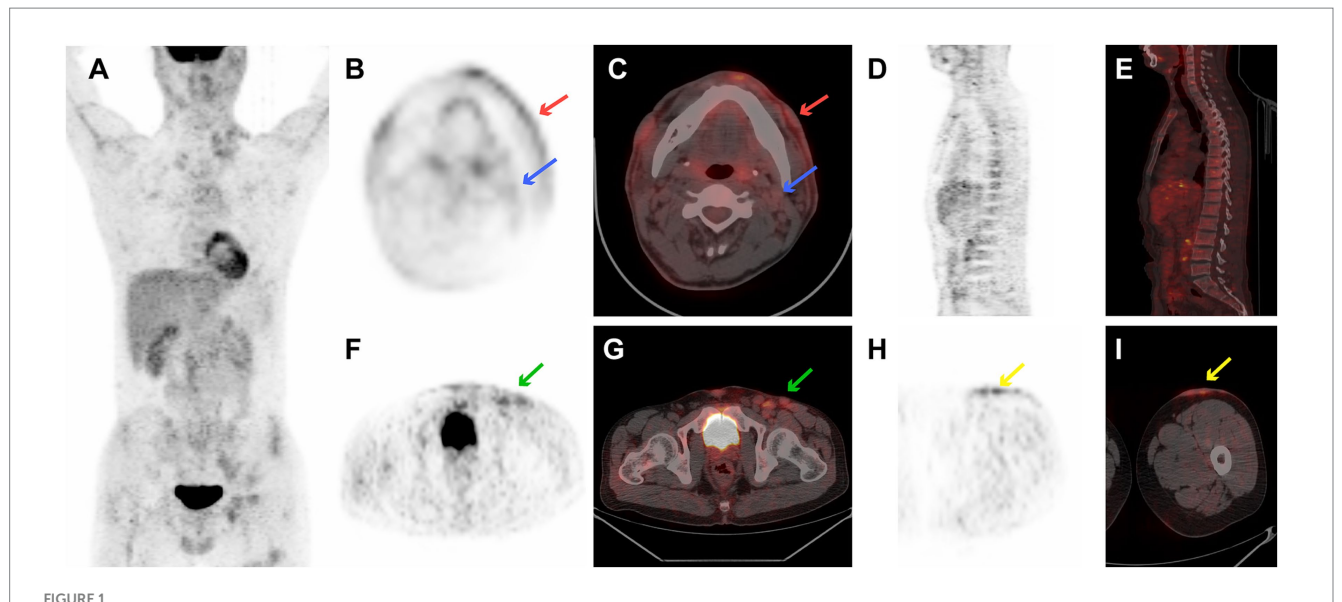
A previously healthy 26-year-old woman presented to our dermatological department with a 6-month history of an asymptomatic dark, violaceous, infiltrated nodular lesion on the left cheek. Physical examination revealed no other obvious abnormalities. Hematology and bone marrow examinations were normal. A skin biopsy of the lesion confirmed the disease as BPDCN. $^{18}\text{F-FDG PET/}$ CT revealed a 3.0 \times 5.5 cm lesion on the left cheek with moderate FDG accumulation at an SUV $_{\text{max}}$ of 2.8 (the SUV of the liver was measured as 3.0). Although the patient received multiple chemotherapeutic regimens, she experienced bone marrow infiltration and died 1 year after diagnosis.

Case report 3

A 51-year-old woman presented with left cervical lymphadenopathy for more than 2 months, which was diagnosed as BPDCN on biopsy. She had undergone a hysterectomy for fibroids 10 years ago. Physical examination revealed multiple enlarged lymph nodes on the bilateral sides of the neck and clavicle areas. A complete blood count was normal. No neoplastic cells were detected in the bone marrow. $^{18}\text{F-FDG}$ PET/CT revealed moderate-to-high FDG-avid cervical and clavicular lymphadenopathy with an SUV $_{\text{max}}$ of 6.8 (SUV of the liver was measured as 3.7). She experienced post-chemotherapeutic bone marrow suppression after one cycle of vincristine, daunorubicin, cyclophosphamide, L-asparaginase, and prednisone (VDCLP) treatment and died 10 days after starting therapy.

Case report 4

A 36-year-old man presented with a 5-month history of a nodular violaceous rash on the skin and multiple lymphadenopathies. He had no specific medical history. Physical examination revealed multiple nodules over his head, neck, chest, and back, and in the left femoral region, together with multiple enlarged lymph nodes in the bilateral neck, bilateral armpits, left groin, and bilateral supraclavicular areas. complete blood count revealed pancytopenia (hemoglobin = 58 g/L, white blood cell = 3.2×10^{-9} /L, and platelet = 4×10^{9} /L). ¹⁸F-FDG PET/CT image is illustrated in Figure 1. Figure 1 shows the ¹⁸F-FDG PET/CT images of case 4, with disseminated cutaneous, lymph nodes, and extranodal localization disease (Figure 1A). ¹⁸F-FDG PET/CT revealed multiple mild-tomoderate FDG-avid cutaneous lesions on his head, neck, chest, and back, and in the left femoral region with an SUV_{max} of 2.6 (the SUV of the liver was measured at 2.7). Supra- and infra-diaphragmatic



¹⁸F-FDG PET/CT images of case 4 revealed multiple mild-to-moderate FDG-avid cutaneous lesions on the head, neck, chest, back, and left femoral region with an SUV_{max} of 2.6. There are supra- and infra-diaphragmatic abnormally enlarged lymph nodes with an SUV_{max} of 3.7. Mild FDG-avid of trunk bone was detected with a SUVmax 1.5. (A) PET maximum intensity projection (MIP), (B) transverse PET image of cutaneous lesion of cheek (red arrows) and cervical lymph nodes (blue arrow), (C) transverse fused PET/CT image of cervical cutaneous lesion of cheek (red arrows) and cervical lymph nodes (blue arrow), (D) sagittal PET image of bone, (E) sagittal fused PET/CT image of bone, (F) transverse PET image of left inguinal lymph nodes (green arrow), (G) transverse fused PET/CT image of left inguinal lymph nodes (green arrow), (H) transverse PET image of cutaneous lesion in left femoral region (yellow arrows), and (I) transverse fused PET/CT image of cutaneous lesion in left femoral region (yellow arrows).

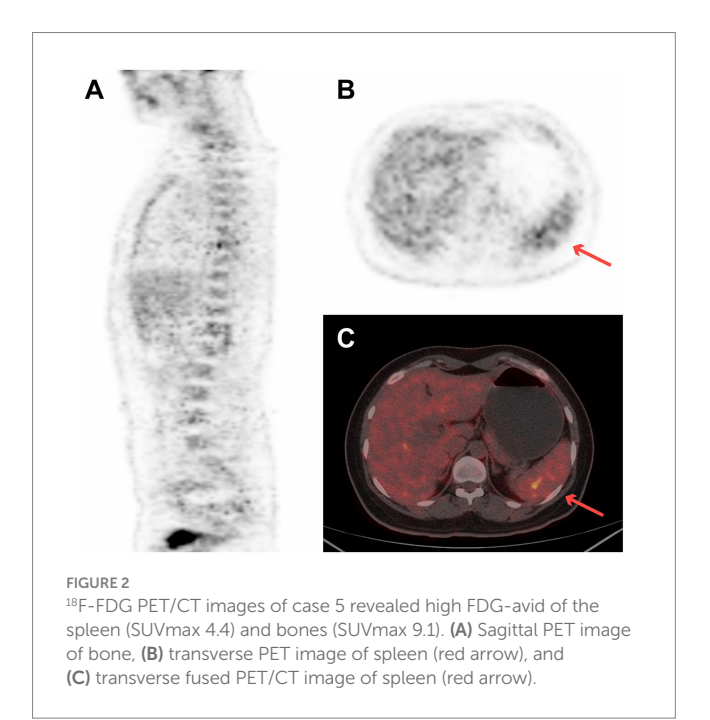
abnormally enlarged lymph nodes were seen in cervical, supraclavicular, axillary, mediastinal, retroperitoneal, and left bilateral inguinal areas with an SUV_{max} of 3.7 (Figures 1B,C,F–I). Mild FDG-avid in the trunk bone was detected with an SUV_{max} of 1.5 (Figures 1D,E). This patient underwent a skin biopsy, cervical lymph node biopsy, and bone marrow examination, all of which indicated BPDCN. He died from gastrointestinal bleeding due to abnormal coagulation function 15 days after diagnosis.

Case report 5

A 27-year-old woman with a 2-week history of back pain was admitted to our orthopedics department. The complete blood count revealed thrombocytopenia (platelet count = $58 \times 10^9/L$). Physical examination revealed scattered ecchymosis on the skin. Figure 2 shows images of case 5 with bone marrow and spleen involvement. $^{18}\text{F-FDG}$ PET/CT revealed high FDG-avid lesions of the bones (SUV $_{\rm max}$, 9.1, Figure 2A) and spleen (SUV $_{\rm max}$, 4.4, Figures 2B,C). No clear lesions were detected at any other sites. This patient underwent a bone marrow examination, and the disease was confirmed as BPDCN. She died of disseminated intravascular coagulation 20 days after diagnosis.

Discussion

In this article, we present five cases of BPDCN diagnosed with ¹⁸F-FDG PET/CT assistance. Subsequently, we performed a systematic literature review using the Web of Science and PubMed databases between January 2000 and July 2023. Combination



search terms included "blastic plasmacytoid dendritic cell neoplasm," "18F-fluorodeoxyglucose-positron emission tomography/computed tomography," "PET/CT," and "PET." The inclusion criteria were: (a) patients diagnosed with BPDCN confirmed by pathologic examination of skin and lymph node or bone marrow biopsy and (b) patients underwent ¹⁸F-FDG PET/CT for initial staging at diagnosis. The exclusion criteria were patients

with a previously diagnosed malignant condition. Finally, 12 articles (including 13 cases) were retrieved (7, 8, 12-21) from the databases.

From March 2014 to July 2023, five patients (cases 1-5) were diagnosed with BPDCN and underwent ¹⁸F-FDG PET/CT for initial staging in Qilu Hospital of Shandong University. We identified 12 studies (including 13 cases) describing ¹⁸F-FDG PET/CT features at diagnosis of BPDCN (7, 8, 12-21). Data collected from our cases and cases in the literature included age, sex, extent of lesion involvement, biopsy site, immunophenotype, treatment, prognosis, and ¹⁸F-FDG PET/CT features. Treatments were categorized as acute myeloid leukemia (AML)-like, acute lymphoblastic leukemia (ALL)-like, or non-Hodgkin lymphoma (NHL)-like chemotherapy regimens, peripheral blood stem cell transplant (PBSCT), radiotherapy, and new drug (SL401) or palliative treatment. Prognosis was defined as overall survival (OS). OS was defined as the time from the first diagnosis of BPDCN to the last follow-up or death. SPSS 24.0 software (SPSS, Inc., Chicago, IL) was used for statistical analyses. The mean age of the cohort is expressed as the median (25-75th percentile). The survival curves were performed using the Kaplan-Meier method.

BPDCN, an extremely rare and aggressive tumor, is derived from precursor plasmacytoid cells. Most patients present with cutaneous lesions, followed by systemic dissemination involving lymph nodes and extranodal localizations (4). Therefore, it is necessary to seek accurate imaging methods for detecting systemic involvement. Given that a single examination can observe lesions and their metabolism throughout the whole body, ¹⁸F-FDG PET/CT has been considered a reliable method for detecting hematopoietic malignancy and plays a vital role in staging and clinical decision-making, especially in the treatment of lymphoma (22). For BPDCN, ¹⁸F-FDG PET/CT is an effective examination method because of the heterogeneity of the affected organs.

Together with our 5 cases, 18 cases of BPDCN containing PET/ CT manifestations were reported (7, 8, 12-21). The clinical features are listed in Table 1. The study included 11 male and 7 female patients. The mean age of our cohort was 35.5 years (17.5–74.8), ranging from 8 to 87 years. The disease was limited to skin (3/18), cutaneous isolated and lymph nodes (1/18), cutaneous isolated and non-cutaneous extranodal localization (1/18), disseminated with cutaneous localization (3/18), disseminated with lymph nodes (1/18), disseminated with lymph node and non-cutaneous extranodal localization (2/18), disseminated with cutaneous, lymph node, and extranodal localization (5/18), and disseminated with non-cutaneous extranodal localization (2/18). Karyotype data were available in five patients, and only one presented with a calreticulin (CALR, Exon9) mutation. The CALR-mutated case (case 14) showed particularly aggressive PET/CT features (multifocal lesions, SUVmax 9.1). This aligns with emerging evidence of molecular heterogeneity in BPDCN (23), though our dataset is underpowered for formal correlation analysis. Furthermore, 15 of 18 patients provided phenotypic information, and 8 of them had a combination of CD4+, CD56+, and CD123+. Three of them revealed a negative expression of CD56.

Although the clinical features and pathology establish the diagnosis of BPDCN, it is crucial to recognize the PET/CT features that can characterize the extent of disease involvement. However, no study has summarized the imaging manifestations of BPDCN, and evidence of the application value of BPDCN is lacking. A reported

international survey of 398 adult patients indicated that 89% of them had skin involvement, either a single mass or multiple scattered skin lesions (4). ¹⁸F-FDG PET/CT results in BPDCN, including our case series and cases in the literature (7, 8, 12-21), are depicted in Table 2. ¹⁸F-FDG uptake was mildly to significantly increased in lesions in all 18 cases (SUV_{max}, 9.1; range, 1.5–9.1). The positive findings of ¹⁸F-FDG PET/CT mainly included skin (11/18), lymph nodes (9/18), bone (4/18), and spleen (2/18). Four cases (57.1%) had high uptake of FDG in bone among seven cases with bone marrow infiltration confirmed by bone marrow biopsy. Except for these organs, abnormal ¹⁸F-FDG uptake lesions were detected in the lung (1/18; SUV_{max}, 5.6) and breast (1/18; SUV_{max}, 1.9). A summary of SUV_{max} values in ¹⁸F-FDG PET/CT of BPDCN is depicted in Table 3. For cutaneous isolated lesions, the FDG uptake was moderate-to-high (range, 2.8-6.7). However, for multiple cutaneous lesions, the FDG uptake was mild-to-moderate (range, 1.5-2.6). Moderate-to-high uptake was observed in lymph nodes (range, 2.3-6.8). For two patients with bone marrow infiltration having PET/CT data, the SUV_{max} of bone was 1.5 and 9.1, respectively. In our study, the single mass or skin lesion manifested as high FDG uptake with a range of 2.8-6.7. The FDG uptake level in multiple skin lesions was relatively low, manifested as a low-to-moderate FDG-avid (range, 1.5-2.6). Besides metabolism-related information, the simultaneous CT images also provided a more accurate measurement of lesion depth and thickness than physical examination (24). Moreover, PET/CT could detect deeper lesions, which were otherwise invisible. The combination of the two provided more useful imaging information. However, the resolution of the PET scan may miss patches and thin plaques, and the partial volume effect may lead to the underestimation of the FDG uptake (24). The imaging feature is also non-specific (12); hence, it is sometimes necessary to consider other clinical manifestations comprehensively.

The ability of PET/CT to detect more lymph nodes involved in lymphoma compared with CT alone was confirmed by a previous study. The metabolic information of PET may help identify the lymph nodes that do not fulfill size criteria (25). Furthermore, 39% of patients with BPDCN had lymph node lesions (4). Our study revealed moderate-to-high FDG-avid lymph node lesions (range, 2.3–6.8); complete metabolic remission was seen after treatment in five patients. PET could distinguish benign lymph nodes from involvement by comparing the FDG uptake values before and after treatment. Furthermore, staging with PET/CT rather than CT could easily detect subcentimetric lymph nodes and assess the extent of nodal involvement (12, 13, 19).

Furthermore, 62% of patients with BPDCN experienced bone marrow infiltration (4). However, only four cases (57.1%) in our study had high uptake of FDG in bone among the seven cases with a positive marrow aspirate. Given the reported sensitivity of PET for detecting marrow involvement in non-Hodgkin lymphoma, positive bone marrow involvement is not always evident on ¹⁸F-FDG PET (26). This serves as a reminder that imaging alone may underestimate bone marrow infiltration, and a bone marrow biopsy should be necessary in the initial evaluation.

As observed in case number 10, the patient had plaques on the right cheek, and ¹⁸F-FDG PET/CT incidentally detected a hypermetabolic breast lesion with proven BPDCN involvement. This discovery changed the patient's treatment strategy, and she remains in complete remission without relapse at 34 months since the initial

frontiersin.org

TABLE 1 Clinical characteristics of 18 patients with BPDCN.

| Patient no. | Age/ sex | Forms | Biopsy site | Karyotype | Immunophenotype | | | | Type of | Prognosis | Ref. | |
|----------------|-------------|--|--|-----------|---------------------------------|---|-----------------------------------|---------------------------------------|--|------------|--------------------------------------|--------|
| | | | | | BPDC markers | T-lymphoid and natural killer cell markers | B-lymphoid markers | Myeloid and monocyte markers | Immature and other markers | treatment | | |
| 1 | 82/M | Disseminated with cutaneous localization | Skin (back) | NA | CD123(+), CD56(+), CD4(+) | CD2(-), CD3(-), CD8(-) | CD20(-) | MPO(-), CD117(-) | CD30(-), TdT(-) | AML-like | PFS: 10 m. | Case 1 |
| 2 | 26/F | Cutaneous isolated | Skin (left cheek) | NA | CD123(+), CD56(+), CD4(+) | CD2(+) | CD79a(-) CD20(-) | NA | CD30(-), CD34(-), CD43(+), TdT(-) | NHL-like | OS:1.2 m. | Case 2 |
| 3 | 51/F | Disseminated with lymph nodes | Left cervical lymphadenopathy | NA | CD123(-), CD56(+), CD4(+) | CD3(-), CD5(-) | CD20(-), CD79a(-) | NA | CD10(-), Bcl-2(+), TdT(+) | ALL-like | OS: 1.6 m. | Case 3 |
| 4 | 36/M | Disseminated cutaneous, lymph nodes, and extranodal localization | skin (chest), bone marrow, left inguinal lymph node | NA | CD123(+), CD56(-), CD4(+) | CD3(-), CD5(-) | CD79α(+)CD20(−) | MPO(-) | CD43(+), S100(-), TdT(-) | Palliative | OS: 0.5 m. | Case 4 |
| 5 | 27/F | Disseminated non- cutaneous extranodal localization | Bone marrow | NA | NA | NA | NA | NA | NA | Palliative | OS: 1 m. | Case 5 |
| 6 | 34/M | Disseminated with cutaneous localization | Cutaneous mass (left lower leg) | NA | CD123(+), CD56(+), CD4(+) | CD3(-) | CD20(-) | MPO(-) | CD30(-) | NA | NA | (12) |
| 7 | 9/M | Disseminated cutaneous, lymph nodes, and extranodal localization | cutaneous mass (right foot) | NA | CD56(+), CD4(+) | NA | NA | NA | NA | NA | CR after 3.8 months of follow-up | (13) |
| 8 | 35/F | Disseminated lymph nodes and non- cutaneous extranodal localization | Axillary lymph node | NA | CD56(-), CD4(+) | CD3(-) | CD20(-), CD79a(-), CD138(-) | MPO(-) | CD30(-), CD43(+), TdT(-) | Palliative | OS: 0.3 m. | (14) |
| 9 | 19/M | Cutaneous isolated | Left elbow | NA | CD56(+), CD4(+) | CD3(-) | CD20(-)CD79a(-) CD138(-) | CD68(+), MPO(-) | CD30(-), CD34(-), CD43(+), TdT(+) | ALL-like | CR after 9 months of follow-up | (14) |

frontiersin.org

TABLE 1 (Continued)

| Patient no. | Age/ sex | Forms | Biopsy site | Karyotype | | ı | mmunophenoty | ре | | Type of | Prognosis | Ref. |
|----------------|-------------|--|--|---------------------------|---------------------------------|---|------------------------------|---|--|--|---|------|
| | | | | | BPDC markers | T-lymphoid and natural killer cell markers | B-lymphoid markers | Myeloid and monocyte markers | Immature and other markers | treatment | | |
| 10 | 47/F | Cutaneous isolated and non-cutaneous extranodal localization | Right cheek, breast | Normal | CD56(+), CD4(+) | CD3(-) | CD20(-) | CD68(+), MPO(-) | CD10(-), CD34(-), Bcl2(+), TdT(+) | ALL-like+ PBSCT | CR after 34 months of follow-up | (8) |
| 11 | 87/F | Disseminated lymph nodes and non- cutaneous extranodal localization | Bone marrow | Normal | CD123(+), CD56(-), CD4(+) | cCD3(-), CD2(+), CD7(+) | NA | CD36(+) | CD34(-) CD38(-) HLA-DR (+) | AML-like | OS: 6 m. | (15) |
| 12 | 82/F | Disseminated non- cutaneous extranodal localization | Lung, bone marrow | Normal | CD123(+), CD56(+), CD4(+) | CD3(-) | NA | NA | CD45RA(+), D34(-), CD38(+), CD43(+) | Multiple chemotherapeutic regimens | OS: 3 m. | (7) |
| 13 | 13/M | Cutaneous isolated | Left cheek | NA | CD123(+), CD56(+), CD4(+) | CD3(-), CD8(-) | CD20(-)PAX5(-) | MPO(-) | CD10(-), TdT(-) | ALL-like | Good response after 9 months of follow-up | (16) |
| 14 | 67/M | Disseminated cutaneous, lymph nodes, and extranodal localization | Skin(chest), inguinal lymph node, bone marrow | CALR (Exon9) L367fs*46 | CD123(+), CD56(+), CD4(+) | Granzyme B(-), CD2(-), CD7(-) | CD20(-)CD138(-) | MPO(-), CD68(-), CD117(-) | CD3(-), CD34(-), CD43(+), TdT(+) | ALL-like | OS:12 m. | (17) |
| 15 | 9/M | Cutaneous isolated and lymph nodes | Skin (left forearm) | NA | CD123(+), CD56(+), CD4(+) | CD1a(-), CD3(-), CD5(-), CD7(-), CD8(-) | CD79a(+)PAX5(-), CD20(-), | MPO(-), CD14(-), CD15(-), CD33(-), CD68(-), CD117(-) | CD10(-), CD34(-), CD45(+), TdT(+) | NHL-like+ALL-like | CR after 15 months of follow-up | (18) |
| 16 | 8/M | Disseminated cutaneous, lymph nodes, and extranodal localization | Skin (left calf) | NA | NA | NA | NA | NA | NA | chemotherapy | Good response after 4 months of follow-up | (19) |
| 17 | 77/M | Disseminated with cutaneous localization | Skin (left forearm and right shoulder) | Normal | CD123(+), CD56(+), CD4(+) | CD1a(-) | CD20(-) | MPO(-) | S-100(-) | Radiotherapy | NA | (20) |

Ref. (21)3 months of CR after reatment SL401 Ϋ́ ΝA mmunophenotype B-lymphoid markers ΝA ΝA markers Ä Karyotype ΝA Biopsy site Ϋ́ nodes, and extranodal cutaneous, lymph Disseminated ocalization Forms 74/M 18

(Continued)

NA, not available; RFS, relapse-free survival; OS, overall survival; AML, acute myeloid leukemia; ALL, acute lymphoblastic leukemia; NHL, non-Hodgkin lymphoma; PBSCT, peripheral blood stem cell transplant; CR, complete remission

diagnosis (8). Therefore, PET/CT may have remarkable advantages in detecting potential lesions in the whole body and providing guidance on biopsy location.

The data regarding treatment were available for 15 patients. Treatment consisted of NHL-like chemotherapy in one patient, ALL-like regimens in four patients, AML-like regimens in two patients, and ALL-like treatment, followed by PBSCT in one patient, multiple chemotherapeutic regimens in two patients, radiotherapy in one patient, SL401 in one patient, and palliative treatment in three patients. A total of 7 of 18 cases reported the follow-up data of PET/ CT, revealing metabolic reduction or remission after treatment. In a clinical trial regarding the activity of SL-401 in patients with BPDCN, ¹⁸F-FDG PET/CT was performed before treatment, after 1 month, and then every 3 months and at times of disease progression (21), demonstrating that ¹⁸F-FDG PET/CT might serve as a tool in the efficacy evaluation and follow-up of BPDCN. As shown in Hodgkin lymphoma, higher PET parameters at baseline were associated with a poor prognosis (27). Prognostic data were available for 16 patients in our cohort. The median OS in this cohort was 12.0 months (range: 0.5-34 months), and the median follow-up time was 10.0 months (Figure 3). Among these, 10 cases reported SUV_{max} of lesions at the same time. Interestingly, five cases out of eight patients with $SUV_{max} > 2.5$ died within 2 months of diagnosis, whereas two other cases with SUV_{max} < 2.5 survived within 10 and 34 months of follow-up. In our BPDCN study, we observed that patients with $SUV_{max} > 2.5$ might experience early death. This suggested that SUVmax might be associated with the prognosis of BPDCN. This study was novel in reporting that FDG uptake might be associated with BPDCN prognosis. However, the data were not sufficient for further statistical analysis.

Scholars suggested that CT or PET/CT should be included in the initial evaluation of a patient with suspected BPDCN (3). In our cases and reported cases, ¹⁸F-FDG PET/CT played a vital role in initial staging (18/18), selection of biopsy sites (5/18), and treatment evaluation (7/18). Seven cases had follow-up data using ¹⁸F-FDG PET/CT (2, 13, 15, 18-21), which showed that during treatment evaluation or clinical follow-up, ¹⁸F-FDG PET/CT could assess disease remission through the resolution of hypermetabolic lesions or absence of disease (Table 2). In our study, ¹⁸F-FDG uptake substantially increased in lesions in all 18 cases, indicating a sensitivity of 100%. Few studies summarized the CT findings of BPDCN (7, 18), and no study focused on 18F-FDG PET/CT imaging features of BPDCN. However, the number of cases included in our study was relatively small due to the low incidence rate of the disease. The institutional and literature-derived data were collected retrospectively, which may introduce potential biases and incomplete data. Irrespective of its advantages over either PET or CT alone, PET/CT is an ideal imaging technique for detecting BPDCN involvement. Additional studies should be performed to address the usefulness and cost-effectiveness of 18F-FDG PET/CT in the clinical practice of BPDCN.

Conclusion

Our case series and cases from the literature demonstrated the utility of ¹⁸F-FDG PET/CT in the diagnosis, staging, prognosis, and treatment follow-up of BPDCN. Early recognition of this rare

TABLE 2 $\,^{18}\text{F-FDG}$ PET/CT features of BPDCN and role in clinical practice.

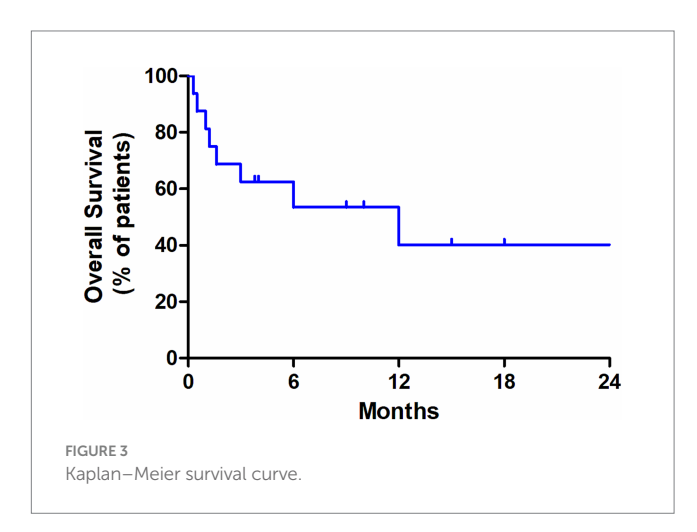
| Patient no. | ¹⁸ F-FDG PET/CT findings at initial (SUVmax) | ¹⁸ F-FDG PET/CT for treatment response or recurrence | Role of ¹⁸ F-FDG PET/ CT | Ref. |
|----------------|--|--|---|--------|
| 1 | Mild FDG-avid cutaneous lesion on the arm, chest, and back (SUVmax 1.5) | | Initial staging | Case 1 |
| 2 | Moderate FDG-avid lesion in the left cheek (SUVmax 2.8) | Resolution of the hypermetabolic lesion in the left cheek (6 weeks after the pretreatment) | Initial staging; Treatment evaluation | Case 2 |
| 3 | High FDG-avid cervical and clavicular lymphadenopathy (SUVmax 6.8) | | Initial staging | Case 3 |
| 4 | Multiple mild-to-moderate FDG-avid cutaneous lesions on his head, neck, chest, back, and left femoral region (SUVmax 2.6) Moderate-to-high FDG-avid supra- and infra-diaphragmatic abnormally enlarged lymph nodes (SUVmax 3.7) Mild FDG-avid of trunk bone (SUVmax 1.5) | | Initial staging Guide biopsies | Case 4 |
| 5 | Diffuse accumulation in spleen (SUVmax 4.4) High FDG-avid of bone (SUVmax 9.1) | | Initial staging Guide biopsies | Case 5 |
| 6 | Multiple mild FDG-avid cutaneous lesions on the back, with involvement of the left inguinal lymph node Markedly increased FDG-avid subcutaneous mass in the left lower leg (SUVmax 6.7) | | Initial staging | (12) |
| 7 | FDG avid soft tissue mass on the dorsal aspect of the right foot (SUVmax 4.1) Metastatic disease of the ipsilateral inguinal and iliac lymph nodes Osseous lesion in the contralateral distal femur | Complete interval resolution of the hypermetabolic inguinal and iliac lymphadenopathy and the osseous lesion | Initial staging, Treatment evaluation | (13) |
| 8 | Nasal mass, cervical, abdominal, axillary, and mediastinal lymphadenopathy | | Initial staging | (14) |
| 9 | Metabolically active disease involving the anteromedial aspect of the left elbow | | Initial staging | (14) |
| 10 | Mild FDG-avid lesion on the right cheek (SUVmax 2.2) Hypermetabolic mass lesion in the right breast (SUVmax 1.9) | | Initial staging; Guide biopsies | (8) |
| 11 | Supra- and infra-diaphragmatic abnormally enlarged lymph nodes Diffuse accumulation in bone and spleen | Complete metabolic remission (after the third cycle of association) | Initial staging; Treatment evaluation | (15) |
| 12 | Elevated FDG uptake in bilateral lungs consistent with interstitial lesions (SUVmax 5.6) | | Initial staging Guide biopsies | (7) |
| 13 | Hypermetabolic activity localized on the left cheek (SUVmax 4.68) | | Initial staging | (16) |
| 14 | Multiple mild FDG-avid cutaneous lesions and involvement of lymph nodes and trunk bone | | Initial staging; Guide biopsies | (17) |
| 15 | Hypermetabolic thickening of the soft tissue in the left forearm and bilateral group 2 cervical lymph nodes Significant metabolic reaction of the left axillary lymph node. | Nearly completely eradicated (following six courses of intensive chemotherapy) No tumor recurrence was detected on PET/CT (15 months after diagnosis). | Initial staging; Treatment evaluation | (18) |
| 16 | FDG uptake within multiple enlarged lymph nodes in the left inguinal, left internal iliac, and left para-aortic regions | Resolution of the hypermetabolic lymphadenopathy (4 weeks after the pretreatment). | Initial staging; Treatment evaluation | (19) |
| 17 | Accumulation was present in the skin of the left forearm (SUVmax 3.5) | These inguinal nodes regressed and were no longer PET-avid (1 month after treatment). | Initial staging; Treatment evaluation | (20) |
| 18 | Enlarged and FDG-avid left inguinal node (SUVmax 3.5) and right inguinal node (SUVmax 2.3) | Absence of disease on PET/CT imaging after treatment | Initial staging; Treatment evaluation | (21) |

 $\ensuremath{\mathsf{SUVmax}}$, maximum standardized uptake value; NA, not available.

TABLE 3 Summary of SUVmax in ¹⁸F-FDG PET/CT of BPDCN, including our data and literature data.

| Organ | Number of lesions | SUVmax | | |
|-----------------|-------------------|---------------------|--|--|
| Skin (single) | 5 | 6.7 (range 2.8–6.7) | | |
| Skin (multiple) | 3 | 2.6 (range 1.5–2.6) | | |
| Lymph nodes | 4 | 6.8 (range 2.3–6.8) | | |
| Bone marrow | 2 | 9.1 (range 1.5–9.1) | | |
| Spleen | 1 | 4.4 (range 4.4) | | |
| Breast | 1 | 1.9 (range 1.9) | | |
| Lung | 1 | 5.6 (range 5.6) | | |
| Sum | 17 | 9.1 (range 1.5–9.1) | | |

SUVmax, maximum standardized uptake value



malignancy on imaging can expedite diagnosis and facilitate early treatment.

Data availability statement

The raw data supporting the conclusions of this article will be made available by the authors, without undue reservation.

Ethics statement

The studies involving humans were approved by Ethics committee of Qilu Hospital of Shandong University. The studies were conducted in accordance with the local legislation and institutional requirements.

References

- 1. Chaperot L, Bendriss N, Manches O, Gressin R, Maynadie M, Trimoreau F, et al. Identification of a leukemic counterpart of the plasmacytoid dendritic cells. *Blood*. (2001) 97:3210–7. doi: 10.1182/blood.V97.10.3210
- 2. Arber DA, Orazi A, Hasserjian R, Thiele J, Borowitz MJ, Le Beau MM, et al. The 2016 revision to the World Health Organization classification of myeloid neoplasms and acute leukemia. *Blood*. (2016) 127:2391–405. doi: 10.1182/blood-2016-03-643544

The participants provided their written informed consent to participate in this study. Written informed consent was obtained from the individual(s) for the publication of any potentially identifiable images or data included in this article.

Author contributions

YZ: Funding acquisition, Writing – original draft. KL: Data curation, Investigation, Writing – review & editing. XJ: Data curation, Investigation, Writing – review & editing. LY: Data curation, Investigation, Writing – review & editing. HZ: Writing – original draft. XL: Methodology, Supervision, Writing – review & editing.

Funding

The author(s) declare that financial support was received for the research and/or publication of this article. This study was supported by the Natural Science Foundation of Shandong Province (ZR2022QH315).

Conflict of interest

The authors declare that the research was conducted in the absence of any commercial or financial relationships that could be construed as a potential conflict of interest.

Generative AI statement

The authors declare that no Gen AI was used in the creation of this manuscript.

Any alternative text (alt text) provided alongside figures in this article has been generated by Frontiers with the support of artificial intelligence and reasonable efforts have been made to ensure accuracy, including review by the authors wherever possible. If you identify any issues, please contact us.

Publisher's note

All claims expressed in this article are solely those of the authors and do not necessarily represent those of their affiliated organizations, or those of the publisher, the editors and the reviewers. Any product that may be evaluated in this article, or claim that may be made by its manufacturer, is not guaranteed or endorsed by the publisher.

- 3. Sangeetha V, Selena Z, Siraj M, Lane AA, Mascarenhas J. Blastic plasmacytoid dendritic cell neoplasm–current insights. *Clin Lymph Myeloma Leuk*. (2001) 19:545–54. doi: 10.1016/j.clml.2019.06.002
- 4. Laribi K, Materre ABD, Sobh M, Cerroni L, Petrella T. Blastic plasmacytoid dendritic cell neoplasms: results of an international survey on 398 adult patients. Blood Adv. (2020) 4:4838–48. doi: 10.1182/bloodadvances.2020002474

- Albiol N, Novelli S, Mozos A, Pratcorona M, Sierra J. Venetoclax in relapsed/ refractory blastic plasmacytoid dendritic cell neoplasm with central nervous system involvement: a case report and review of the literature. J Med Case Rep. (2021) 15:326. doi: 10.1186/s13256-021-02939-7
- Zandi S, Ghaffar H. Blastic plasmacytoid dendritic cell neoplasm in ocular adnexa. Blood. (2022) 140:1656. doi: 10.1182/blood.2022017308
- 7. Endo K, Mihara K, Oiwa H, Yoshida T, Mino T, Sasaki N, et al. Lung involvement at initial presentation in blastic plasmacytoid dendritic cell neoplasm lacking cutaneous lesion. *Ann Hematol.* (2013) 92:269–70. doi: 10.1007/s00277-012-1557-4
- 8. Lee HJ, Park HM, Ki SY, Choi YD, Yun SJ, Lim HS. Blastic plasmacytoid dendritic cell neoplasm of the breast a case report and review of the literature. *Medicine*. (2021) 100:4. doi: 10.1097/md.0000000000025699
- 9. Djurdjevic P, Todorovic Z, Jovanovic D, Cekerevac I, Antic D. Blastic plasmacytoid dendritic cell neoplasm of the uterus. *Srp Arh Celok Lek.* (2020) 148:27. doi: 10.2298/SARH191111027D
- 10. Ter-Pogossian MM, Phelps ME, Hoffman EJ, Mullani NA. A positron-emission transaxial tomograph for nuclear imaging (PETT). *Radiology*. (1975) 114:89–98. doi: 10.1148/114.1.89
- 11. Salem AE, Shah HR, Covington MF, Koppula BR, Fine GC, Wiggins RH, et al. Pet-ct in clinical adult oncology: I. Hematologic malignancies. *Cancer.* (2022) 14:5941–75. doi: 10.3390/cancers14235941
- $12.\,Li$ ZG, Mu HY. Blastic plasmacytoid dendritic cell neoplasm evaluated by FDG PET/CT. Clin Nucl Med. (2017) 42:551–2. doi: 10.1097/rlu.0000000000001665
- 13. Martineau P, Pelletier-Galarneau M, Turpin S, Lambert R. Imaging pediatric plasmacytoid dendritic cell neoplasm with FDG PET/CT: atypical presentation of a rare disease. *Clin Nucl Med.* (2016) 41:426–7. doi: 10.1097/rlu.0000000000001159
- 14. Purkait S, Gupta S, Bakhshi S, Mallick S. Blastic plasmacytoid dendritic cell neoplasm: a clinicopathological diagnostic dilemma report of three cases with review of literature. *J Cancer Res Ther.* (2022) 18:S471–4. doi: 10.4103/jcrt.JCRT_420_20
- 15. Le Calloch R, Arnaud B, Le Clech L, Hutin P, Salmon F, Ottou FG, et al. Achievement of rapid complete remission in an 87-year-old female patient with azacytidine-venetoclax for blastic plasmacytoid dendritic cell neoplasm. *Ann Hematol.* (2022) 101:1347–9. doi: 10.1007/s00277-021-04718-2
- 16. Rivas-Calderon MK-W, OrlyRosas-Romero MET-C, Duran-Mckinster S. CarolaGonzalez-Pedroza, et la. Primary cutaneous blastic plasmacytoid dendritic cell neoplasm in a child: a challenging diagnosis and management. *Pediatr Dermatol.* (2021) 38:260–2. doi: 10.1111/pde.14473

- 17. Yan M, Wang W, Cen X, Wang L, Sun Y, Wang B, et al. Blastic plasmacytoid dendritic cell neoplasm with a history of cytopenia: a case report. *Diagn Cytopathol.* (2020) 48:1102–6. doi: 10.1002/dc.24463
- 18. Phusuphitchayanan P, Vejjabhinanta V, Takpradit C, Sudtikoonaseth P, Chairatchaneeboon M, Kiatvichukul T, et al. A rare case of blastic plasmacytoid dendritic cell neoplasm in a child mimicking lymphoma/leukemia cutis. *Dermatopathology*. (2022) 9:321–6. doi: 10.3390/dermatopathology9040038
- 19. Nizza D, Simoneaux SF. Blastic plasmacytoid dendritic cell neoplasm presenting as a subcutaneous mass in an 8-year-old boy. *Pediatr Radiol.* (2010) 40:40–2. doi: 10.1007/s00247-010-1731-6
- 20. Ishibashi N, Maebayashi T, Aizawa T, Sakaguchi M, Sugitani M. Radiation therapy for cutaneous blastic plasmacytoid dendritic cell neoplasm: a case report and review of the literature. *Int J Clin Exp Med.* (2015) 8:8204–9.
- 21. Frankel AE, Woo JH, Ahn C, Pemmaraju N, Rowinsky E. Activity of SL-401, a targeted therapy directed to interleukin-3 receptor, in blastic plasmacytoid dendritic cell neoplasm patients. *Blood.* (2014) 124:385–92. doi: 10.1182/blood-2014-04-566737
- 22. Cheson BD. Role of functional imaging in the management of lymphoma. *J Clin Oncol.* (2011) 29:1844–54. doi: 10.1200/jco.2010.32.5225
- 23. Khoury JD, Solary E, Abla O, Akkari Y, Alaggio R, Apperley JF, et al. The 5th edition of the World Health Organization classification of Haematolymphoid Tumours: myeloid and histiocytic/dendritic neoplasms. *Leukemia*. (2022) 36:1703–19. doi: 10.1038/s41375-022-01613-1
- 24. Kuo PH, Mcclennan BL, Carlson K, Wilson LD, Edelson RL, Heald PW, et al. FDG-PET/CT in the evaluation of cutaneous T-cell lymphoma. *Mol Imaging Biol.* (2008) 10:74–81. doi: 10.1007/s11307-007-0127-y
- 25. Tsai EY, Taur A, Espinosa L, Quon A, Johnson D, Dick S, et al. Staging accuracy in mycosis fungoides and sezary syndrome using integrated positron emission tomography and computed tomography. *Arch Dermatol.* (2009) 142:119–20. doi: 10.1001/archderm.142.5.577
- 26. Pakos EE, Fotopoulos AD, Ioannidis JPA. 18F-FDG PET for evaluation of bone marrow infiltration in staging of lymphoma: a meta-analysis. *J Nucl Med.* (2005) 35:958–63. doi: 10.1590/S0100-06832011000500022
- 27. Louarn N, Galicier L, Bertinchamp R, Lussato D, Montravers F, Oksenhendler EPR, et al. First extensive analysis of F-18-labeled fluorodeoxyglucose positron emission tomography-computed tomography in a large cohort of patients with HIV-associated hodgkin lymphoma: baseline total metabolic tumor volume affects prognosis. J Clin Oncol. (2022) 40:1346–55. doi: 10.1200/jco.21.01228